Distinct nanostructures from isomeric molecules of bis(iminopyrrole) benzenes: effects of molecular structures on nanostructural morphologies†

Yaobing Wang,[ab] Hongbing Fu,*[a] Aidong Peng,[a] Yongsheng Zhao,[ab] Jinshi Ma,[a] Ying Ma[a] and Jiannian Yao*[a]

Received (in Cambridge, UK) 29th January 2007, Accepted 8th March 2007
First published as an Advance Article on the web 23rd March 2007
DOI: 10.1039/b701327b

The effects of molecular structures on nanostructural morphologies have been studied through the preparation of nanospheres, square nanowires, and nanocubes from three isomeric molecules of bis(iminopyrrole)benzene.

Recent researches on organic nanoparticles (ONPs) demonstrated that not only can the wide panel of physical properties provided by functional compounds be fully exploited, but the properties can also be modulated by the particle size and shape.[1–3] However, although tailor-made molecules can generally be obtained by organic synthesis, ensuring that the molecules aggregate in a specific way and thus generate nanostructures with a desirable size, shape, and therefore function, remains a great challenge.[4] This is because molecule components are easily trapped in kinetically stable arrangements of varying topology. The ability to understand and predict the complex nanostructural morphology lies in understanding how the specific structures of interacting molecules encode information about the final geometry of the organized objects. This is also a central topic in fields such as supramolecular chemistry,[4,5] organic and protein crystallization,[6] and biomineralization.[7]

Manipulation of particle morphology by altering the initial molecular geometry of the compound being precipitated has been met with limited success.[8] Our group have fabricated uniformly shaped organic nanorods and nanospheres by the self-aggregation of different stilbazolium-like dyes.[2b] Zang and co-workers have prepared nanobelts and nanospheres from different derivatives of perylene diimide.[3] In both cases, the molecular structure of the target dye compound is modified by the introduction of long alkyl chains. Therefore, the dominant driving forces for molecular aggregation are turned from strong π–π interactions between dye molecular cores to hydrophobic interactions between alkyl chains, leading to the formation of organic nanostructures with distinct shapes. Herein, we report nanostructures with well-defined shapes, such as sphere, square wire, and cube, prepared from three isomeric molecules of bis(iminopyrrole)benzene. Although all three isomeric precursors present similar strong multiple hydrogen-bonding interactions for molecular aggregation, distinctly shaped nanostructures are obtained. It is the different interactions for aggregate stacking at supramolecular level caused by the isomeric molecular structures that is most likely responsible for the different morphological evolution.[9]

Model compounds of isomers of *o*-, *m*- and *p*-bis(iminopyrrole) benzene are synthesized by condensation of *o*-, *m*- and *p*-phenylenediamines with 2-carboxaldehyde pyrrole in high yields.[10] The crystal structures of these compounds are shown in Fig. 1 as **a**, **b** and **c**, respectively.‡ All three isomeric molecules are semi-rigid and almost full conjugated with characteristic configurations. The angles between the long axes of two iminopyrroles (IP) groups on phenyl ring are 60°, 120°, and 180°, in compounds **a**, **b** and **c**, respectively. Moreover, the two IP groups, which can rotate to some extent, point in opposite directions, up and down, divided by the central phenyl plane. It can be seen from Fig. 1 that each molecule contains four complementary hydrogen-bonding sites in two IP subunits: the two imine N atoms act as acceptors and the two pyrrolic NH groups act as donors.

Self-assembled nanoscale structures with distinct morphologies are fabricated by the deposition of target compounds from a saturated solution onto clean substrates. In a typical preparation, the substrates are immersed in saturated solutions of precursors in acetonitrile at room temperature. Then the temperature is gradually decreased to −5 °C, and kept for several days. To obtain nanostructures with perfect morphology, the speed of cooling is very important to assure an equilibrium-based organizational process so that the precursors are neither trapped

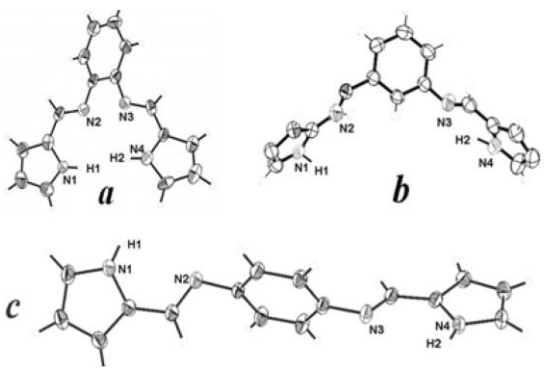

Fig. 1 ORTEP drawings of compounds **a**, **b** and **c**, respectively, with 50% probability ellipsoids for non-hydrogen bonding atoms. The N and H atoms forming the hydrogen bonds are labelled with black symbols.

[a]*Beijing National Laboratory for Molecular Sciences (BNLMS), Institute of Chemistry, Chinese Academy of Sciences, Zhongguancun, Beijing, 100080, P.R. China. E-mail: hongbing.fu@iccas.ac.cn; jnyao@iccas.ac.cn; Fax: +86-10-82616517; Tel: +86-10-82616517*
[b]*Gradate School of Chinese Academy of Science, Beijing, 100039, P.R. China*

† Electronic supplementary information (ESI) available: Related synthetic experiments, crystallography and SEM image details; full references 1–3. See DOI: 10.1039/b701327b

in kinetically stable arrangements of varying topology nor form the bulk crystals easily. Scanning electron microscopy (SEM) results reveal that compounds **a** and **c** generate spherical and cubic nanoparticles as shown in Fig. 2A and C, respectively, while compound **b** forms nanowires with a square shaped cross-section (Fig. 2B). The diameter of the nanospheres and the side length of the nanocubes are around 400 and 300 nm, respectively. The side length of the square cross-section of the nanowires is around 300 nm, but the length of nanowires adds up to several micrometres. These crystalline nanowires display moderate mechanical flexible property, which is in sharp contrast with the macroscopic crystalline materials (see Figure S4†). Nanostructures of compound **a**–**c** are also successfully deposited on carbon film and imaged by transmission electron microscopy (TEM). As shown in Fig. 2, the overall morphologies observed by TEM are quite the same as those observed by SEM. Note that (i) all the preparation conditions for the nanostructures are identical for compounds **a**–**c**; (ii) similar results are observed by using different substrates. Therefore, we conclude that the distinct morphologies of self-assembled nanostructures are intrinsically related to the molecular structures of compounds **a**–**c**.

To characterize the molecular packing in the solid state, single crystal X-ray diffraction (XRD) analysis is performed in detail for compounds **a**–**c**.‡ Two IP groups in compound **a** are 60° open-armed. Therefore, two monomers of **a** can embed into each other and form a dimer *via* quadruple hydrogen bonds, in which no additional sites are available for further hydrogen bonding. These dimers are the actual building blocks (see Fig. S1†) for solid state, and are brought together *via* van der Waals interactions. Single-crystal analysis of **a** reveals that two kinds of dimer are required to form a unit crystal cell. In contrast with **a**, the configurations of **b** and **c**, with two IP groups open-armed at an angle of 120° and 180°, respectively, determine that every molecule has to connect with two different molecules by hydrogen-bonding, forming a chain-like structure. Also determined by molecular configurations, the chain of **b** is zigzag shape (see Fig. S2†) while that of **c** is almost linear (see Fig. S3†). These chains are the actual building blocks for solid state of **b** and **c**.

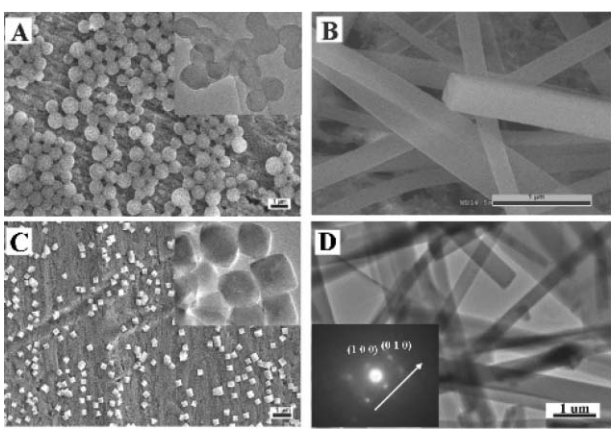

Fig. 2 SEM images of (A) nanospheres, (B) square nanowires and (C) nanocubes, fabricated from compounds **a**, **b** and **c**, respectively. The insets in (A) and (C) show the corresponding TEM images. The inset in (D) of the TEM image of square nanowires depicts the electronic diffraction pattern. All the scale bars are 1 μm.

The comparison between the X-ray diffraction profiles of nanostructures and bulk powder in Fig. 3 provides a clue for us to understand the real picture of molecular packing at nanoscale regime. In each panel of Fig. 3, stick plot represents the bands simulated by using of the program of DIAMOND based on the single-crystal structure data. It can be seen that the diffraction peaks observed for nanostructures and bulk powder can be perfectly indexed to the single-crystal data. For compound **a**, there are no characteristic diffraction peaks detectable for nanospheres. This indicates that the nanospheres are amorphous as a result of the randomly packing of **a** dimers. As the above mentioned crystals of **a** are built by two kinds of dimers held together by a multitude of van der Waals interactions. The amorphous nature of the nanospheres means that the collective magnitude of van der Waals interactions at the nanoscale is too weak to ensure perfect crystal packing. In contrast to the case of the nanospheres fabricated by **a**, there are characteristic diffraction peaks detectable for nanowires (Fig. 3B) and nanocubes (Fig. 3C) fabricated by **b** and **c**, respectively. Fig. 3C shows that for compound **c** the diffraction profile of the nanocubes is almost the same as that of the powder. However, for compound **b**, a distinct peak corresponding to (010) plane is clearly observed in the diffraction profile of the nanowire, but is not observed in that of powder (Fig. 3B). This, plus the ED pattern of square nanowires in TEM measurements (see the inset of Fig. 2D) suggest that molecules of **b** within the nanowires prefer to arrange themselves along the crystal (010) direction.

Why does preferential crystal growth occur for **b** nanowires but not for **c** nanocubes? In order to correlate the molecular structures to the morphologies of nanostructures, we propose a mechanism in Fig. 4. In our systems and similarly to the process of protein folding[11] as well as the growth of fibrillar structures,[12] the

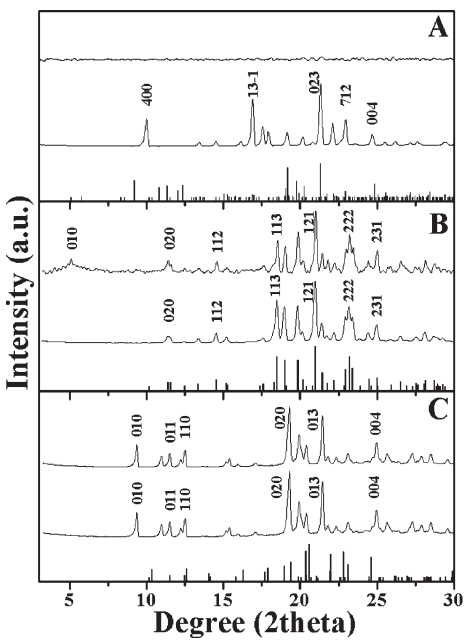

Fig. 3 XRD patterns of self-assembled nanostructures (above), powder (middle), and simulated bands (below) of compound **a**, **b** and **c**, respectively. The simulation has been performed by using of the program of DIAMOND based on the single-crystal structure data.

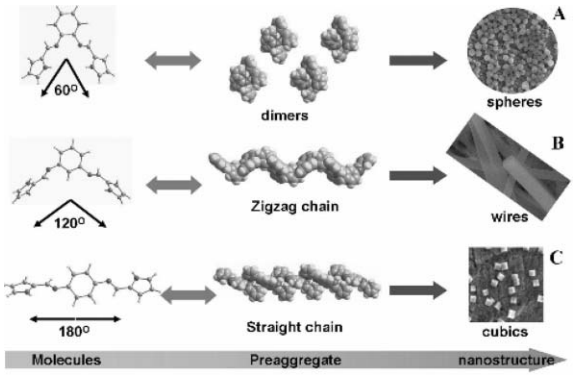

Fig. 4 The schematic representation for the formation processes of nanoscale materials of compounds **a**, **b** and **c**, respectively. See text for details.

formation of an organized object requires several steps: (i) formation of preaggregates (primary), (ii) association of preaggregates (secondary), and (iii) conversion into the final structure (tertiary).[11,13] Compound **a** forms dimers as the preaggregate, which are quasi-spherical (see the middle image in Fig. 4A). The weak and diffuse nature of van der Waals driving forces for the association of dimers leads to the formation of amorphous nanospheres. Unlike **a**, preaggregates for **b** and **c** should be the zigzag and linear hydrogen-bonded chains (see the middle images in Fig. 4B and 4C). Although aggregation numbers are unknown in both cases, they are hydrogen-bonding open with two free sites at each end. Therefore, association of chain-like preaggregates can occur either by direct lock-in of existing preaggregates *via* hydrogen-bonding interactions or by side-by-side stacking of hydrogen-bonded chains *via* van der Waals interactions. In the case of **b**, the zigzag shape of chain-like preaggregate provides more molecular contacts as recognition sites favourable for the latter path (see Fig. S2c and S2d†). On the one hand, side-by-side stacking of hydrogen-bonded chains facilitates the molecules in the preaggregates become more restricted in relative position, necessary for the formation of organized structure, for example, crystal structure. On the other hand, larger is the aggregate generated by side-by-side stacking, more hydrogen-bonding sites does the aggregate provide and thus larger is its hydrogen-bonding association constant. Therefore, association of preaggregates for **b** is a cooperative process, according to a very recent publication by Jonkheijm and co-workers.[12] The ED and XRD pattern of square nanowires indicate that the nanowire is growing along the crystal (010) direction, coincident with the direction of **b** zigzag hydrogen-bonded chains. In the case of **c**, lack of recognition sites (see Fig. S3c and S3d†) make the association of **c** linear chains less cooperative, thus nanocubes rather than square nanowires are formed. At one time, the side-by-side stacking of chain-like preaggregates are considered to be against the direct linkage in the assembling process of one-dimensional nanomaterials.[14] Our results indicate that the growth along the direction of preaggregates has been in cooperation with the side-by-side stacking of preaggregates to obtain one-dimensional morphology.

In conclusion, we successfully prepared nanospheres, square nanowires, and nanocubes from three isomeric molecules respectively. We found that molecular structures not only decide the primary hydrogen-bonding geometries of preaggregates, but also influence the secondary association of preaggregates, and therefore the final morphologies of nanostructures. Essentially, hierarchical intermolecular interactions may have different effects and play different roles at different level of size regime. (i) To get organic nanocrystalline, strong intermolecular interactions, such as π–π, hydrogen-bonding, has to survive at supramolecular level. (ii) The cooperation of the growth along the direction of preaggregates with the side-by-side stacking of preaggregates is necessary to obtain one-dimensional morphology.

This work was supported by the National Natural Science Foundation of China (Nos 90301010, 50573084, 90606004), the Chinese Academy of Sciences (“100 Talents” program), and the National Research Fund for Fundamental Key Project 973 (2006CB806200, 2006CB932101).

Notes and references

‡ Crystal data for **a**: $C_{16}H_{14}N_4$, Mr = 262.31, monoclinic, space group *C*2/*c*, a = 34.919(7) b = 17.106(3) c = 14.362(3) Å, β = 93.49(3)°, V = 8562.86(1593) Å^3, β_{calcd} = 1.22076 g cm^{-3}. Crystal data for **b**: $C_{16}H_{14}N_4$, Mr = 262.31, orthorhombic, space group *Pbca*, a = 10.2048(10) b = 15.5662(15) c = 17.4159(17) Å, V = 2766.5(47) Å^3, β_{calcd} = 1.25949 g cm^{-3}. Crystal data for **c**: $C_{16}H_{14}N_4$, Mr = 262.31, monoclinic, space group *P*2(1)/*n*, a = 10.894(2) b = 9.1577(18) c = 14.177(3) Å, β = 90.888(3)°, V = 1414.25(49) Å^3, β_{calcd} = 1.23195 g cm^{-3}. CCDC 299563–299565. For crystallographic data in CIF format see DOI: 10.1039/b701327b

1 H. Kasai, H. Kamatani, S. Okada, H. Oikawa, H. Matsuda and H. Nakanishi, *Jpn. J. Appl. Phys.*, 1996, **35**, L221.
2 (*a*) H. B. Fu and J. N. Yao, *J. Am. Chem. Soc.*, 2001, **123**, 1434; (*b*) Z. Y. Tian, Y. Chen, W. S. Yang, J. N. Yao, L. Y. Zhu and Z. G. Shuai, *Angew. Chem., Int. Ed.*, 2004, **43**, 4060.
3 (*a*) K. Balakrishnan, A. Datar, T. Naddo, J. L. Huang, R. Oitker, M. Yen, J. C. Zhao and L. Zang, *J. Am. Chem. Soc.*, 2006, **128**, 7390; (*b*) K. Balakrishnan, A. Datar, R. Oitker, H. Chen, J. M. Zuo and L. Zang, *J. Am. Chem. Soc.*, 2005, **127**, 10496.
4 (*a*) E. R. Zubarev, E. D. Sone and S. I. Stupp, *Chem.–Eur. J.*, 2006, **12**, 7313; (*b*) R. Iwaura, F. J. M. Hoeben, M. Masuda, A. P. H. J. Schenning, E. W. Meijer and T. Shimizu, *J. Am. Chem. Soc.*, 2006, **128**, 13298.
5 (*a*) D. M. Vriezema, M. C. Aragones, J. A. A. W. Elemans, J. J. L. M. Cornelissen, A. E. Rowan and R. J. M. Nolte, *Chem. Rev.*, 2005, **105**, 1445; (*b*) J. A. A. W. Elemans, R. van Hameren, R. J. M. Nolte and A. E. Rowan, *Adv. Mater.*, 2006, **18**, 1251.
6 (*a*) V. F. Rosenberger, M. P. G. Muschol and B. R. Thomas, *J. Cryst. Growth*, 1996, **168**, 1; (*b*) T. Shimizu, M. Masuda and H. Minamikawa, *Chem. Rev.*, 2005, **105**, 1401.
7 E. Baeuerlein, *Biomineralization*, Wiley-VCH, Weinheim, 2000.
8 (*a*) J. Chad, S. Sarika, S. Bala and A. S. Borovik, *J. Am. Chem. Soc.*, 2005, **127**, 9698; (*b*) M. Oh and C. A. Mirkin, *Nature*, 2005, **438**, 651.
9 (*a*) A. Patra, N. Hebalkar, B. Sreedhar, M. Sarkar, A. Samanta and T. P. Radhakrishnan, *Small*, 2006, **2**, 650; (*b*) Sonika sharma and T. P. Radhakrishnan, *ChemPhysChem*, 2003, **4**, 67.
10 Z. Wu, Q. Chen, S. Xiong, B. Xin, Z. Zhao, L. Jiang and J. S. Ma, *Angew. Chem., Int. Ed.*, 2003, **42**, 3271.
11 (*a*) J. L. Jimenez, E. J. Nettleton, M. Bouchard, C. V. Robinson, C. M. Dobson and H. R. Saibil, *Proc. Natl. Acad. Sci. U. S. A.*, 2002, **99**, 9196; (*b*) A. Aggeli, I. A. Nyrkova, M. Bell, R. Harding, L. Carrick, T. C. B. McLeish, A. N. Semenov and N. Boden, *Proc. Natl. Acad. Sci. U. S. A.*, 2001, **98**, 11857.
12 (*a*) F. Wurthner, V. Stepanenko and A. Sautter, *Angew. Chem., Int. Ed.*, 2006, **45**, 1939; (*b*) P. Jonkheijm, P. V. D. Schoot, P. H. J. Schenning and E. W. Meijer, *Science*, 2006, **313**, 80; (*c*) V. Percec, G. Ungar and M. Peterca, *Science*, 2006, **313**, 55.
13 (*a*) A. Johnson, S. Sharma, B. Subramaniam and A. S. Borovik, *J. Am. Chem. Soc.*, 2005, **127**, 9698; (*b*) H. Maeda, M. Hasegawa, T. Hashimoto, T. Kakimoto, S. Nishio and T. Nakanishi, *J. Am. Chem. Soc.*, 2006, **128**, 10024.
14 K. V. Workum and J. F. Douglas, *Phys. Rev. E*, 2006, **73**, 031502.